Effect of metal coating and residual stress on the resonant frequency of MEMS resonators

ASHOK KUMAR PANDEY, K P VENKATESH and RUDRA PRATAP*

CranesSci MEMS Laboratory, Department of Mechanical Engineering, Indian Institute of Science, Bangalore 560 012
e-mail: pratap@mecheng.iisc.ernet.in

Abstract. MEMS resonators are designed for a fixed resonant frequency. Therefore, any shift in the resonant frequency of the final fabricated structure can be a denting factor for its suitability towards a desired application. There are numerous factors which alter the designed resonant frequency of the fabricated resonator such as the metal layer deposited on top of the beam and the residual stresses present in the fabricated structure. While the metal coating, which acts as electrode, increases the stiffness and the effective mass of the composite structure, the residual stress increases or decreases the net stiffness if it is a tensile or compressive type respectively. In this paper, we investigate both these cases by taking two different structures, namely, the micro cantilever beam with gold layer deposited on its top surface and the MEMS gyroscope with residual stresses. First, we carry out experiments to characterize both these structures to find their resonant frequencies. Later, we analytically model those effects and compare them with the experimentally obtained values. Finally, it is found that the analytical models give an error of less than 10% with respect to the experimental results in both the cases.

Keywords. Resonator; metal coating; residual stress; experimental results; analytical model.

1. Introduction

With the increasing use of microengineering techniques (Madou 1997) in producing sensing and actuating devices, it become increasingly significant to consider various after-effects of these techniques if the devices are expected to perform to their specification. MEMS resonators made of polysilicon have potential application in the areas of RF-MEMS (Senturia 2000), MEMS oscillators (Maluf 2000), resonant sensors such as biological mass detector (Craighead 2000), etc. As a resonator, the most important characteristics are the resonant frequency and the quality factor (Fedder 1994, Rao 1995). Since the MEMS resonators are designed for a fixed resonant frequency, any shift in the resonant frequency of the final fabricated structure can be a denting factor for its suitability towards a desired application. There are numerous

---
*For correspondence

factors which alter the designed resonant frequency of the fabricated resonator. Some of these factors are the metal layer which is deposited on the top of the structural layer and the presence of residual stresses in the fabricated structure. The metal layer coating, which acts as an electrode, increases the stiffness and the effective mass of the composite structure (Chiou & Lin 2005, Zhang *et al* 2005) while the residual stress increases or decreases the net stiffness if it is a tensile or compressive stresses respectively (Zhangt *et al* 1990, Bellout *et al* 1999, Pandey *et al* 2007).

There are many studies which deal with modelling the effect of metal coating and residual stresses on the resonant frequencies of simple devices. Chiou & Lin (2005) have proposed the computation of effective flexural rigidity in the design of a composite cantilever beam. Zhang *et al* (1990) have also found the analytical solution for predicting effective stiffness and residual stresses in multilayered coatings in MEMS structure. Zhangt *et al* (1990) have proposed the resonant frequency technique to find the elastic constants of the silicon beam from the experimental results. The resonant frequency technique has been described in (Bellout *et al* 1999) for fixed-fixed beam to compute elastic constants and residual stresses. The frequency resonant technique for the guided cantilever beam is also presented in (Pandey *et al* 2007).

In this paper, we investigate the effects of metal coating as well as residual stress on the resonance frequencies by taking two different structures. The effect of metal coating is studied by taking a cantilever beam which is fabricated using PolyMUMPs process (MUMPs) as
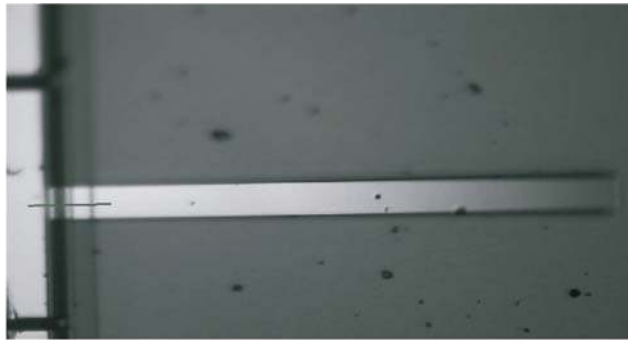
(a)
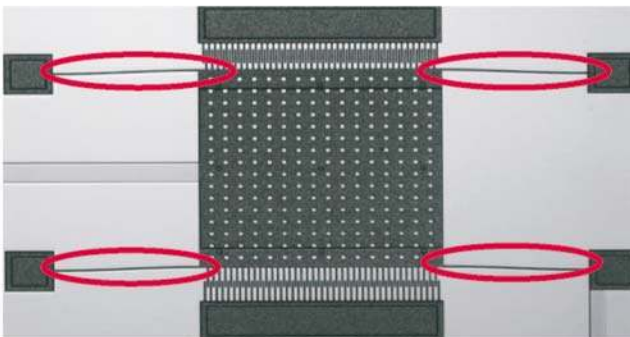
(b)

Figure 1. **(a)** Micro cantilever beam and **(b)** MEMS gyroscope.

Table 1. Geometric dimensions of the structure.

Structure	Parameter	Value
Cantilever	Beam length, l_b	$390\,\mu$m
	Beam width, W_b	$30\,\mu$m
	Poly silicon thickness	$2\,\mu$m (ideal)
	Metal thickness	$0\cdot5\,\mu$m (ideal)
Gyro	Proof mass	$500\times500\,\mu\text{m}^2$
	Beam length, l_b	$300\,\mu$m
	Beam width, W_b	$4\,\mu$m
	Hole size	$10\times10\,\mu\text{m}^2$
	Thickness	$3\cdot5\,\mu$m

shown in figure 1a. The effect of residual stress is studied by taking another MEMS resonator (fabricated using surface micromachining process under different operating conditions) which consists of a proof mass and is supported by four guided cantilever beams as shown in figure 1b. We then characterize both these structures using Polytec Scanning Laser Vibrometer (PSV) — a Polytec product (Polytec) for the out-of-plane motion — to find their resonant frequencies. Finally, we analytically model the effects of metal layer and the residual stress on the resonant frequency for both the structures and then compare the results with the experimental values.

2. Microfabrication process

The PolyMUMPs process (Madou 1997) which is used to fabricate cantilever resonator has different variations in the thickness of the metal and the structural layers, and also the Young's modulus of the polysilicon layer. In this process, the thickness may vary from $1\cdot85\,\mu$m to $2\cdot15\,\mu$m for the polysilicon layer and $0\cdot46\,\mu$m to $0\cdot58\,\mu$m for the metal layer (MUMPs). The structure micro cantilever beam shown in figure 1a is free from residual stresses. Its important dimensions are mentioned in table 1.

Another MEMS structure, shown in figure 1b, is fabricated under different operating conditions. The fabrication of this device also involves the well-known steps of microfabrication (Madou 1997). This structure seems to be affected by the presence of residual stress. This fact can be assessed by observing the SEM image of the fabricated structures on the same silicon wafer in which some of the structures are permanently deflected as shown in figure 1b. The important dimensions of the fabricated structure are mentioned in table 1.

3. Experimental studies

To excite and measure the dynamic characteristics of the structures, we use MSA 400 Microsystem Analyzer — a Polytec product (Polytec) to characterize the out-of-plane vibrations by Scanning Laser-Doppler Vibrometer which works on the principle described in figure 2. The working principle involves electrical excitation which causes the suspended structure to vibrate with respect to the substrate. The measurement laser beam from the interferometer in the scanning head is positioned to a scan point on the object by means of mirrors
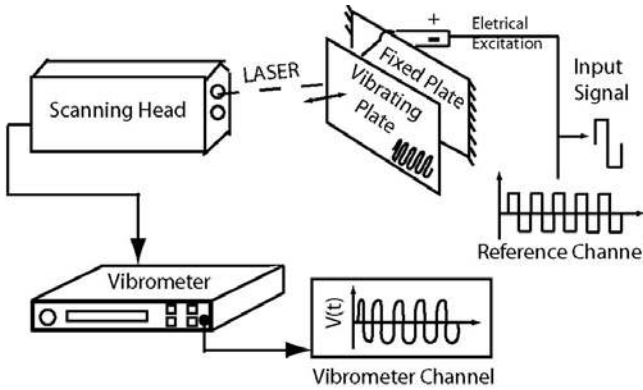
Figure 2. Working principle of test set-up.

and is scattered back. The back-scattered laser light interferes with the reference beam in the scanning head. A photo detector records the interference. A decoder in the vibrometer provides a voltage which is proportional to the velocity of the vibration parallel to the measurement beam. The voltage is digitized and processed as vibrometer signal. Based on the above principle, the measurement details of the micro cantilever beam and micromachined gyroscope are described in the following two sections.

3.1 *Measurements for cantilever beam*

To find the resonant frequencies of the microcantilever structures, we apply 1 V DC and 0·6 V AC pseudorandom signal with frequencies ranging from 1 kHz to 1 MHz. From the captured modes and the frequencies shown in figure 3, the resonant frequencies of cantilever beam of length 390 μm are found and mentioned in table 2. The response curves and the mode shapes corresponding to first five bending modes are also shown in figure 3.

3.2 *Measurements for gyroscope*

To find the resonant frequency corresponding to the out-of-plane mode of the MEMS gyroscope (shown in figure 1b), we apply 4 V DC and 1 V AC pseudorandom signal with frequen-
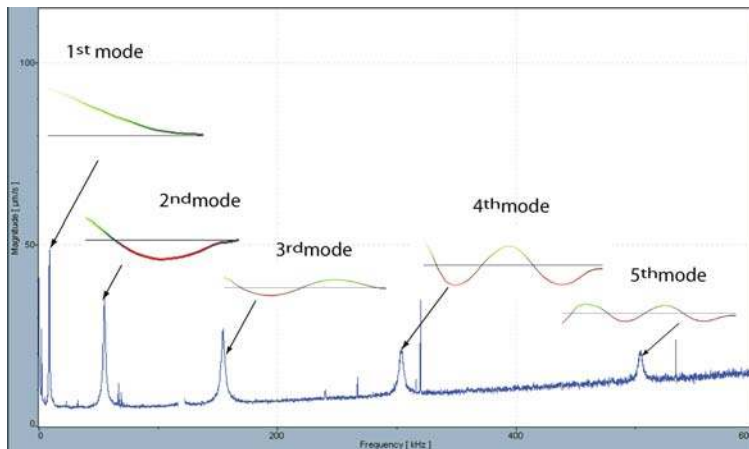

Figure 3. Response of cantilever with gold coating.

Table 2. Experimental results for cantilever beam.

| Mode number	Frequency in kHz
1	8·75
2	54·84
3	154·2
4	304·1
5	504·5

cies ranging from 1 kHz to 40 kHz. The captured mode and the frequency corresponding to the out-of-plane motion are shown in figure 4. The fundamental resonant frequency is found to be 16·9 kHz.

4. Analytical models and their comparison with experimental results

In the first part of the section, we analytically compute the resonant frequency of the cantilever beam which is made of 2 μm thickness polysilicon material and is coated with 500 nm thickness of gold layer. In the second part of the paper, the effect of residual stress is analytically modelled for the MEMS gyroscope. Finally, the analytical results are compared with the experimental results in the corresponding sections.

4.1 *Effect of metal coating*

Figure 3 shows the response of the microcantilever beam which is coated with 500 nm gold layer. In this section, we provide an analytical formulation to model the effect of metal coating on the resonant frequency of a cantilever beam.
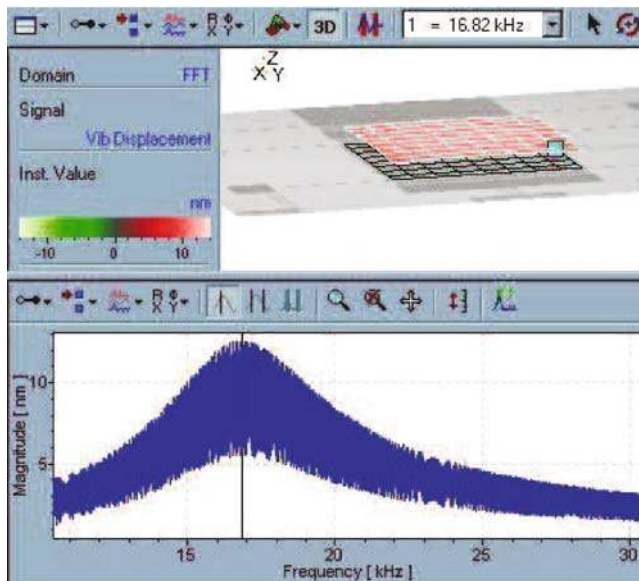
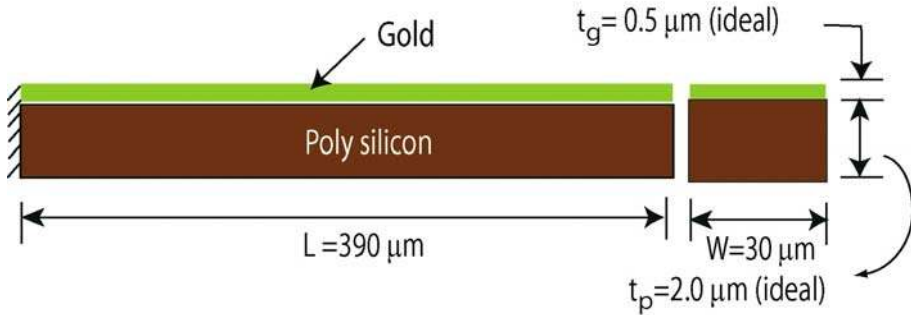**Figure 4.** Frequency response of MEMS gyro.

Figure 5. Polysilicon beam with gold coating.

Figure 5 shows the pictorial representation of polysilicon cantilever beam with a gold coating of 0·5 μm if the fabrication condition is taken as an ideal condition. Since there ought to be the variation in the thickness of the final structure which is fabricated from PolyMUMPs process, the following variations in the thickness of polysilicon and the gold layer are taken into account: 1·85 μm to 2·15 μm with an ideal value of 2·0 μm for polysilicon layer and 0·46 μm to 0·58 μm with an ideal value of 0·52 μm for the gold layer (mumps). Because of different operating conditions of the PolyMUMPs process, the Young's modulus of the polysilicon film is also found to be in the range of 158 ± 10 GPa (mumps). Now, to model the effect of metal coating on resonant frequencies, we start with the computation of effective flexural rigidity of the beam in the subsequent section.

4.1a *Effective flexural rigidity calculations:* Since the displacement about the neutral axis remains the same in both the polysilicon and gold films, it can be treated as two springs in parallel. Let us assume E_P as the Young's modulus of polysilicon and E_g as that of gold. Similarly, I_P as the moment of inertial of polysilicon film about the neutral axis and I_g as that of gold film. Then, the effective flexural rigidity, EI, may be computed from

$$(EI)_{\text{eff}} = E_p I_p + E_g I_g. \tag{1}$$

Therefore, the computation of flexural rigidity of the composite beam involves the determination of moment of inertia of the polysilicon structure and the gold layer about its neutral axis. Referring to figure 6, the effective moment of inertia of the polysilicon beam about the neutral axis of the composite structure is given by:

$$I_p = \frac{Wt_p^3}{12} + Wt_p \left(\frac{H}{2} - \frac{t_p}{2} \right)^2. \tag{2}$$

And that of gold layer is given by

$$I_g = \frac{Wt_g^3}{12} + Wt_g \left(\frac{H}{2} - \frac{t_g}{2} \right)^2. \tag{3}$$

Substituting the values of moment of inertia of polysilicon film and gold film in eqn. (1), we get an effective flexural rigidity for the Young's modulus of polysilicon as $E_p = 160$ GPa and that of gold as $E_g = 77$ GPa. The value of effective Young's modulus of the composite structure is found to be 85·5 GPa for a given $I = \frac{Wt_g^3}{12}$.
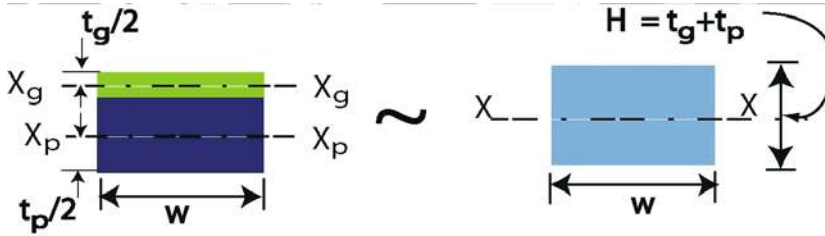
Figure 6. Equivalent beam model for composite beam.

4.1b *Computation of resonant frequency:* The resonant frequency of cantilever beam is given by (Rao 1995):

$$\omega = C\sqrt{\frac{EI}{\rho l^4}}. \tag{4}$$

Where ρ is the linear density (mass per unit length) of a composite beam made of polysilicon and gold layers. It is given by:

$$\rho = \frac{M_{\text{poly Si}} + M_{\text{gold}}}{l}, \tag{5}$$

l is the length of the beam and C is a constant which depends on different modes as mentioned in table 3 (Rao 1995). The values of EI are computed from eqn. (1).

The third column of table 3 presents the first five resonant frequencies f_{wm} of the polysilicon cantilever beam without any metal coating. The fourth column presents the resonant frequency f_m of the composite beam in which the gold layer is deposited on the top of the polysilicon beam. These frequencies are computed from eqn. (4). If we compare the ratio of the frequencies f_{wm} and f_m for different modes, it is found that $f_{wm}/f_m \approx 2 \cdot 2$. This difference is mainly due to a reduction in the effective flexural rigidity and an increase in the effective mass of the system because of gold layer on the top of polysilicon beam resonator.

4.1c *Comparison between analytical and experimental results:* Table 4 compares the analytical and experimental results of the cantilever beam with thickness of $1 \cdot 85 \, \mu$m for

Table 3. Values of C and the resonant frequencies for different modes of the cantilever beam with and without metal coating.

Mode number	C	f_{wm} (in kHz)	f_m (in kHz)
1	3·516	19·7	9·35
2	22·036	123·4	58·63
3	61·697	345·4	164·17
4	120·902	676·8	321·71
5	199·86	1118·9	531·82

Table 4. Comparison between analytical and experimental results.

Mode number	f_{anal}	f_{exp}
1	9·35 kHz	8·75 kHz
2	58·63 kHz	54·84 kHz
3	164·17 kHz	154·2 kHz
4	321·71 kHz	304·1 kHz
5	531·82 kHz	504·5 kHz

polysilicon material and 0·46 μm for gold layer. It is found that the analytical results give an error of less than 5% for first five modes.

If we take an admissible variation in the thicknesses of the polysilicon and gold layers, we get different values of resonant frequencies. Table 5 provides an error between the analytical and experimental results for different thicknesses of composite cantilever beam. It is found that the percentage error of the analytical results may vary from 5% to 22% depending on the admission thickness of the cantilever beam fabricated using PolyMUMPs process.

4.2 *Effect of residual stress*

To study the effect of residual stress, we take MEMS gyroscope. Figure 4 shows the response of MEMS gyroscope structure in its out-of-plane motion. The analytical modelling of this effect in this case may be done by considering the equivalent spring-mass model of the original system. In this structure, the cantilever beams which are used to support the proof mass are assumed to be a guided beam.

In this paper, an approximate value of the fundamental resonant frequency is obtained from the energy method (Rao 1995, Zhangt *et al* 1990). This method equates the kinetic energy due to oscillation with the potential energy due to both deflection and axial stress and then solves for the natural frequency. Rayleigh's quotient (i.e. the ratio of potential energy to kinetic energy) for MEMS gyroscope structure which consists of a proof mass and four axially loaded guided beams is given by (Bellout *et al* 1999, Pandey *et al* 2007):

$$\omega^2 = \frac{4EI \int_0^l \frac{d^2 y}{dx^2} dx + 4\sigma A \int_0^l \frac{d^2 y}{dx^2} dx}{4\rho A \int_0^l y^2 dx + m_{\text{plate}}}, \tag{6}$$

Table 5. Error between analytical and experimental results for different values of polysilicon and gold layers thickness.

t_p	t_g	$[(f_a - f_{\text{exp}})/f_a] \times 100$
1·85 μm	0·46 μm	5 %
2·00 μm	0·52 μm	15%
2·15 μm	0·58 μm	21%

where E is the Young's modulus of the polysilicon material, ρ is the density of polysilicon, I is the area moment of inertia, A is the cross-sectional area, σ is the axial residual stress in the released structure, m_{plate} is the mass of the perforated plate, and $y(x)$ is the mode shape of oscillating beam. Let us assume the mode shape of the guided cantilever beam as (Pandey *et al* 2007):

$$y(x) = \frac{1}{2} - \frac{1}{2}\sin\left(\frac{\pi x}{l}\right). \tag{7}$$

Substituting the mode shape from eqn. (7) in eqn. (6), the simplified form of the first natural frequency of the MEMS gyroscope is given by:

$$\omega^2 = \frac{\pi^4}{2}\frac{EI}{l^3 m_{\text{eff}}} + \frac{\pi^2}{2}\frac{\sigma A}{l m_{\text{eff}}}, \tag{8}$$

where $m_{\text{eff}} = \frac{13}{35}\rho A l + m_{\text{plate}}$ is the effective mass of the structure, $m_{\text{plate}} = 1 \cdot 87\,\mu g$ is the mass of the perforated proof mass. The first term of eqn. (8) is the first natural frequency of the MEMS gyroscope without residual stress.

To compute the residual stress and the resultant Young's modulus in the MEMS structure shown in figure 1b, we consider two different structures A and B. For these structures, $l_A = 300\,\mu m$ and $l_B = 400\,\mu m$ are the length of the guided cantilever beams. The cross-sectional properties, material properties, and residual stresses are same in both the structures. If f_A and f_B are resonant frequencies of the structure A and B, respectively, then the expression for Young's modulus and residual stress can be obtained from eqn. (8):

$$E = \frac{8}{\pi^2 I}\frac{l_A m_{\text{eff}}^A f_A^2 - l_B m_{\text{eff}}^B f_B^2}{\left(\frac{1}{l_A^2} - \frac{1}{l_B^2}\right)} \tag{9}$$

$$\sigma = 8\frac{l_A^3 m_{\text{eff}}^A f_A^2 - l_B^3 m_{\text{eff}}^B f_B^2}{l_A^2 - l_B^2}. \tag{10}$$

Now, for the structure A and B of beam lengths $l_A = 300\,\mu m$ and $l_B = 400\,\mu m$, respectively, the experimental values of the first resonant frequency is obtained as $f_A = 16 \cdot 9\,\text{kHz}$ and $f_B = 14 \cdot 1\,\text{kHz}$. Taking the cross-sectional area $A_{cs} = 14 \cdot 0\,mu m^2$, the area moment of inertia $I = 1 \cdot 42 \times 10^{-23}\,\text{m}^4$ and the density $\rho = 2300\,\text{kg/m}^3$, the values of E and σ are given by:

$$E = 131 \cdot 11\,\text{GPa} \quad \text{and} \quad \sigma = 77 \cdot 71\,\text{MPa}. \tag{11}$$

If we neglect the effect of residual stress in the formula, we end up getting different values of the natural frequency, i.e. $f_{300}^0 = 6 \cdot 74\,\text{kHz}$ and $f_{400}^0 = 4 \cdot 37\,\text{kHz}$ which are an order of magnitude less than the actual values of $16 \cdot 9\,\text{kHz}$ and $14 \cdot 1\,\text{kHz}$, respectively. Therefore, it is essential to include the effect of residual stress developed due to fabrication process in order to predict the actual frequency of the released structure. The difference in the resonant frequency of the stressed and unstressed structures may also be obtained from the numerical simulation in ANSYS as shown in figure 7.
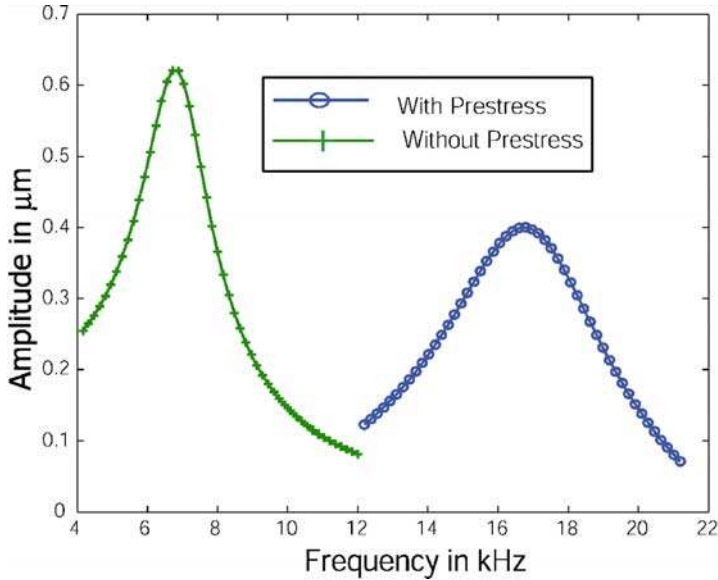
Figure 7.   Shift in resonant frequency due to tensile residual stress.

5. Conclusions

The effect of metal coating on the resonant frequency is studied by taking a MEMS cantilever while the effect of residual stress is studied with MEMS gyroscope. The experiments are performed to find out their resonant frequencies. The analytical models are also presented to model these effects.

For the MEMS cantilever beam which is found to be in unstressed state, the resonant frequency changes by 15% if the thickness of the polysilicon and the gold layers are allowed to change from $1 \cdot 85 \, \mu$m to $2 \cdot 15 \, \mu$m and $0 \cdot 46 \, \mu$m to $0 \cdot 58 \, \mu$m, respectively. Since the Young's modulus of the poly layer is also a variant of the process parameters, the frequency change of 6 to 8% is observed for the Young's modulus of 158 ± 10 GPa. For the polysilicon and metal layers of thicknesses $1 \cdot 85 \, \mu$m and $0 \cdot 46 \, \mu$m, respectively, and the Young's modulus of the polysilicon as 160 GPa, the analytical result gives an error of 5% with respect to the experimental result. In the study of the effect of residual effect, it is found that tensile residual stress of $77 \cdot 71$ MPa changes the natural frequency from $6 \cdot 77$ kHz to $16 \cdot 97$ kHz in MEMS gyroscope. These changes are also verified using numerical simulation in ANSYS.

References

Bellout H, Neustupa J, Penel P 1999 Elastic properties and vibration of micro-machined structures subject to residual stresses. *Proc. IEEE Canadian Conference on Electrical and Computer Engineering*, 1674–1679

Chiou J C and Lin Y J 2005 A novel large displacement electrostatic actuator: Prestress comb drive actuator. *J. Micromech. Microeng.* 15: 1641–1648

Craighead H G 2000 Nanoelectromechanical systems. *Science* 290(5496): pp. 1532–5

Fedder G K 1994 *Simulation of microelectomechanical systems*. Ph.D thesis, University of California.

Madou M 1997 *Fundamentals of microfabrication*, (Florida: CRC Press).

Maluf N 2000 *Introduction to microelectromechanical systems engineering*, (Boston: Artech house)

Pandey A K, Rudra Pratap, Venkatesh K P 2007 Effect of residual stress and perforations on the dynamic characterstics of MEMS devices. *Proc. 1st National Conference of Research Scholars in Mechanical Engineering*, India, 35–40

Polytec reference manual. URL: http://www.polytec.com

Rao S S 1995 *Mechanical Vibrations*, (New York: Wesley Publishing Company)

Senturia S D 2000 *Microsystem Design*, (Boston: Kluwer Academic Publishers)

URL: http://www.memsrus.com/documents/polyMUMPS. rundata.xls

Zhang X C, Xu B S, Wang H D, Wu Y X 2005 An analytical model for predicting thermal residual stresses in multilayer coating. *J. Thin Solid Films* 488: 274–282

Zhangt L M, Zhangt, Uttamchandanit D, Culshawt B, Dobson P 1990 Measurement of Young's modulus and internal stress in silicon microresonators using a resonant frequency technique. *Meas. Sci. Technol.* 1: 1343–1346